Status report on the design of the CLIC post-collision line

Arnaud Ferrari

Department of Nuclear and Particle Physics
Uppsala University, Sweden

CLIC meeting, CERN, 16 June 2006

Introduction (1)

At CLIC, the incoming beams experience very strong electromagnetic fields at the interaction point.

$\rightarrow$ Increased angular divergence of the disrupted beam, emission of beamstrahlung photons (thus a larger energy spread) and production of e^+e^- coherent pairs.

All these particles must be transported to their dump with minimal losses in the extraction line.

In 2005, we studied the beam losses in the 20 mrad extraction line of a TeV collider (upgraded ILC or low-energy CLIC) and we performed some benchmarking studies of tracking codes (DIMAD vs BDSIM).

Introduction (2)

In 2006, we started the design of the CLIC post-collision line, where the beam disruption, beamstrahlung photon emission and coherent pair production are much worse than at ILC.

- Study of the beam losses of a nominal CLIC beam in a scaled 20 mrad ILC post-collision line.
- First design of an extraction chicane, study of the constraints for the post-collision magnets.
- Study of the stress and temperature constraints at the dump window.

Contents

Incoming beam parameters

Parameter	Symbol	Value	Unit
Center-of-mass energy	E	3	TeV
Particles per bunch	N_b	2.56	10^9
Bunches per RF pulse	n	220	
Bunch spacing	Δt_b	0.267	ns
Repetition frequency	f	150	Hz
Primary beam power	P_b	20.4	MW
Horizontal normalized emittance	$(\beta\gamma)\epsilon_x$	660	nm.rad
Vertical normalized emittance	$(\beta\gamma)\epsilon_y$	10	nm.rad
Horizontal rms beam size	σ_x	60	nm
Vertical rms beam size	σ_y	0.7	nm
Rms bunch length	σ_z	30.8	μm
Peak luminosity	L	6.5	10^{34} cm^{-2} s^{-1}

Incoming beam parameters of the nominal CLIC machine [CLIC note 627].

Disrupted beam distributions

Strong beam-beam interactions lead to an emittance growth and the apparition of low-energy tails in the disrupted beam.

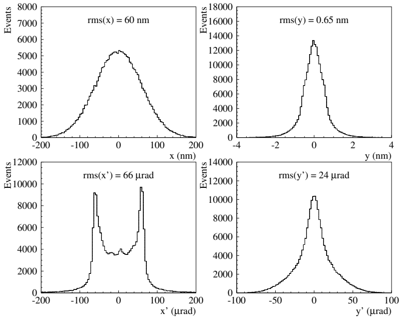

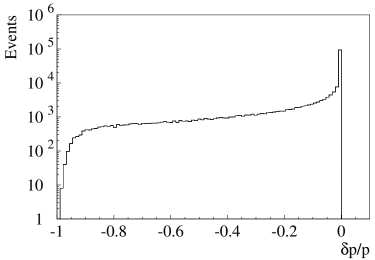

Distributions for CLIC at 3 TeV

Beamstrahlung photons

At CLIC, 1.1 beamstrahlung photons are emitted per incoming electron or positron. The average energy loss of each incoming beam through emission of photons is $\delta_B = 16\%$.

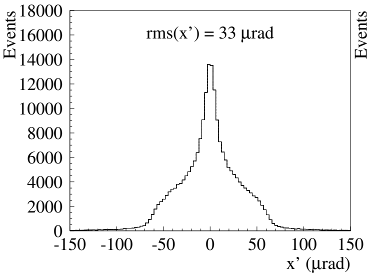

Coherent pairs

At CLIC, one expects 4.6×10^7 coherent pairs per bunch crossing. The electrons and positrons of the coherent pairs carry typically about 10% of the primary beam energy.

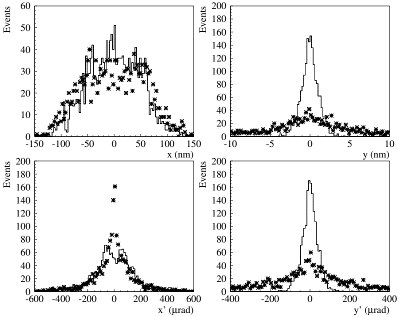

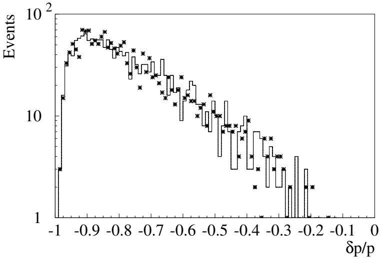

* ↔ wrong-sign charged particles

Outgoing beams with an offset

A vertical offset in position and/or angle (Δy or $\Delta y'$) affects the beam-beam effects, and thus the outgoing beam distributions.

The effects of a vertical offset were derived from numerous GUINEA-PIG simulations. For the design of the post-collision beam line, the most relevant effect is an increase of the vertical angular divergences.

- the largest horizontal/vertical angular divergences of the disrupted beam are about 70/75 μrad,
- the largest horizontal/vertical angular divergences of the beamstrahlung photons are about 40/80 μrad,
- one may expect up to almost 10^8 coherent pairs per bunch crossing (the energy spectrum is unchanged though).

Disrupted beams with an offset

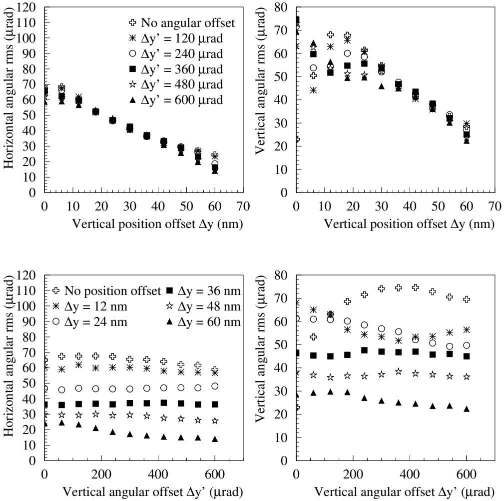

Beamstrahlung photons with an offset

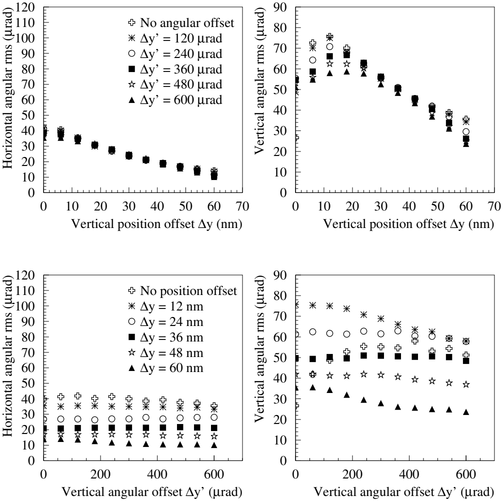

Coherent pairs with an offset

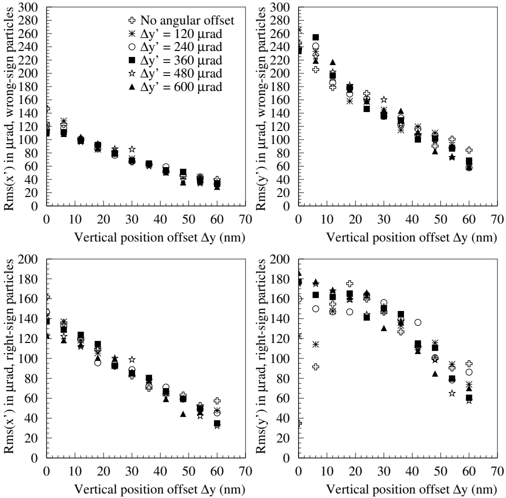

Contents

The ILC 20 mrad extraction line

The ILC 20 mrad extraction line consists of a DFDF quadruplet, followed by two vertical chicanes for energy and polarization measurements and a field-free region with two collimators at 200 and 300 m downstream of the interaction point.

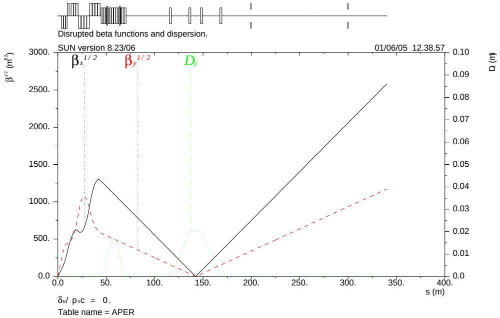

Estimation of the power losses

The disrupted beam distributions are tracked with DIMAD, from the interaction point to the dump.
Using the number of lost particles in the extraction line, as well as their energy, one calculates the total beam power loss:

$$P_{loss}[W] = 1.602 \times 10^{-10} \frac{N_b\, n\, f}{N_{tracks}} \sum_{i=1}^{N_{loss}} E_i \, .$$

- N_b is the number of particles per bunch,
- n is the number of bunches per RF pulse,
- f is the repetition frequency (in Hz),
- N_{tracks} and N_{lost} are the number of tracked and lost particles,
- E_i is the energy of the particle i (in GeV).

Disrupted beam losses (1)

Most of the disrupted beam losses come from the low-energy tail, which tend to be over-focused in the first quadrupoles of the extraction line. The 20 mrad ILC extraction line only accepts primary electrons/positrons with $E_i/E > 40\%$.

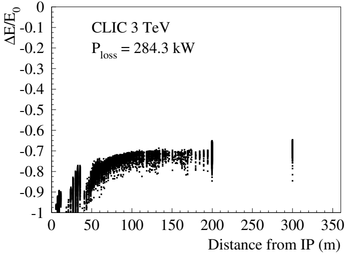

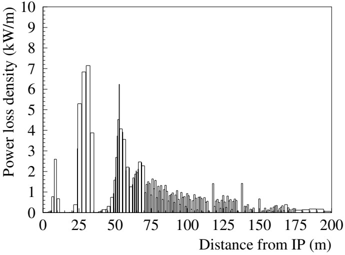

Disrupted beam losses (2)

Magnetic elements	Total beam losses	Maximal loss density
SC Quadrupoles	6.5 kW	2.6 kW/m
Warm Quadrupoles	61.5 kW	7.1 kW/m
Energy Chicane Magnets	48.0 kW	4.5 kW/m
Polarimetry Chicane Magnets	0.8 kW	0.4 kW/m

Total beam losses and maximal loss density in the first section of the ILC 20 mrad extraction line (upstream of the collimators) for CLIC at 3 TeV.

As for the beam losses in the two round collimators, we find 87.8 kW in COLL1 and 11.4 kW in COLL2.

Power losses for the coherent pairs

About 80% of the particles coming from the coherent pairs do not reach the dump. These power losses mostly occur due to the over-focusing of low-energy particles in the quadrupoles and do not depend on the charge.

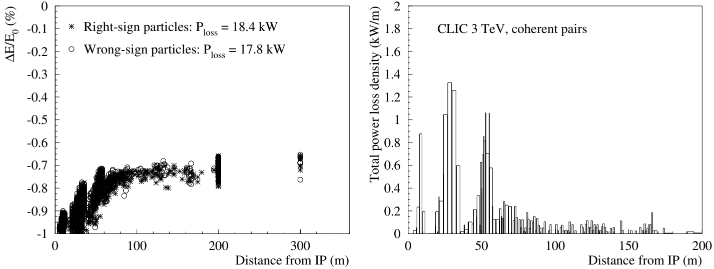

Power losses vs magnet settings

Scaling down the magnetic fields in all dipoles and quadrupoles by f_{QB} is equivalent to changing the central energy of the beam, thus effectively reducing the total energy spread and allowing transmission of more particles.

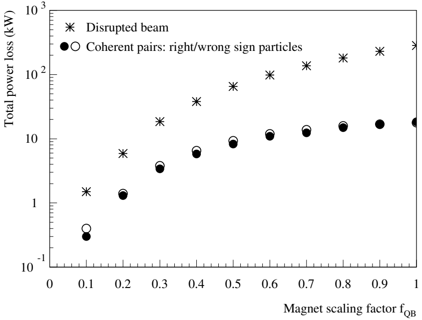

Extraction line optics with new magnet settings (1)

One should reduce all magnetic fields by at least a factor five to reach a reasonable level of power losses. Even so, the power deposited in the SC quadrupoles is still a few hundred Watts.

Also, the optics of the 20 mrad extraction line at the nominal energy is destroyed when changing all magnetic fields in the dipoles and quadrupoles.

The optics condition for a secondary focus point is no longer fulfilled at the nominal energy.

Extraction line optics with new magnet settings (2)

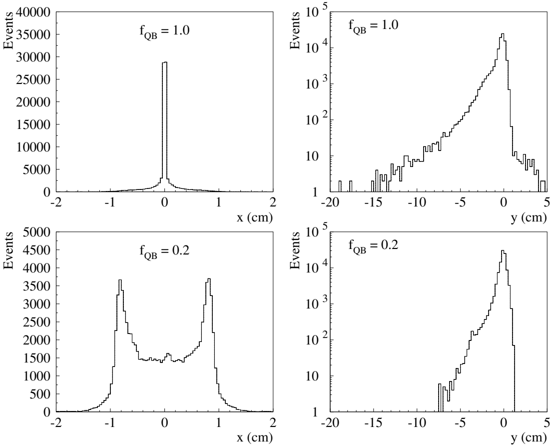

Conclusions

- A detailed study of the beam losses along the ILC 20 mrad extraction line was performed, with nominal CLIC beams.
- The power losses are mostly due to the low-energy tails of the disrupted beams and the coherent pairs, over-focused in the first quadrupoles of the post-collision line.
- The ILC 20 mrad extraction line is thus not adapted to the nominal CLIC beam, due to large losses (280 kW for the disrupted beam and 36 kW for coherent pairs).
- A strong reduction of all dipolar and quadrupolar fields allows to bring the power losses down to a reasonable level. On the other hand, the optics of the post-collision line is destroyed at the nominal energy.

Contents

Conceptual design

The proposed design of the CLIC post-collision line is based on the separation by dipole magnets of the disrupted beam, the beamstrahlung photons and the particles of the coherent pairs that have the wrong-sign charge as compared to the outgoing beam, just downstream of the interaction point.

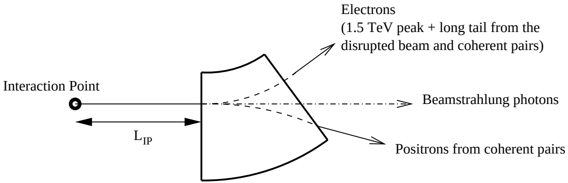

It should then be followed by a transport to the dump through dedicated extraction lines.

Some constraints on the magnet design

We use window-frame magnets for the CLIC post-collision line:

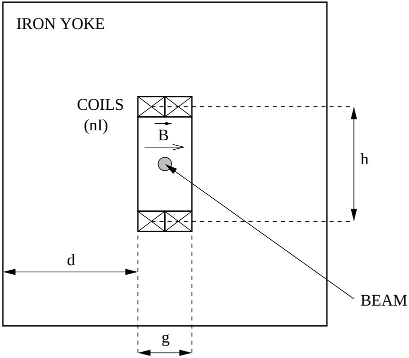

Ampere's law:

$$nI = \oint \mathbf{H} \cdot d\mathbf{s} \simeq \frac{B}{\mu_0} g$$

For the magnetic flux to return through the yoke:

$$d \geq \frac{\Phi/2}{\ell B_{max}} \Longrightarrow d \geq h \times \frac{B}{2B_{max}}.$$

Some constraints for e/γ vertical separation

For particles with a momentum p_0 of 1.5 TeV/c, we want that the vertical deviation δy_0 is 5 times larger than the worse rms photon cone size at the exit of the dipole [rms$^\gamma$(y') = 80 μrad, with offset].

$$\theta\ [\text{mrad}] = 0.8 \times \left(1 + \frac{L_{IP}}{L_D}\right) \text{ and } \theta\ [\text{mrad}] = 0.2 \times BL_D\ [\text{T.m}]$$

$$BL_D^2 - 4L_D - 4L_{IP} = 0 \Longrightarrow L_D = \frac{2}{B}\left(1 + \sqrt{1 + L_{IP}B}\right).$$

The field strength B should typically be of the order of 1 T. We choose $L_{IP} = 24$ m to ensure that the post-collision extraction magnet is outside the detector. One thus gets L_D =12 m, for a vertical bending angle of 2.4 mrad at 1.5 TeV.

Estimation of the pipe and magnet dimensions (1)

The conceptual design that we propose here is based on three post-collision magnets, with a length of 4 m and spaced by 1 m.

The horizontal beam size increases linearly with the distance to the interaction point. The most stringent constraint for the gap comes from the coherent pairs: rms(x') reaches 0.15 mrad.

$$X_{pipe}(z)\ [\mathrm{cm}] \geq 0.15 \times z\ [\mathrm{m}].$$

Magnet	nI (A)	X_{coil} (cm)	Y_{coil} (cm)
1	4.14×10^4	5.2	16.0
2	4.77×10^4	6.0	16.0
3	5.41×10^4	6.8	16.0

Obtained with a current density of 10 A/mm^2, assuming that half of the coil cross section is used for cooling.

Estimation of the pipe and magnet dimensions (2)

In the vertical direction, one must perform particle trackings to estimate the beam size in the magnets.

In the first post-collision magnet, one must reduce the beam losses as much as possible (direct line-of-sight to the detector for the secondary particles). Meanwhile, one needs a compact magnet (close incoming beam line).

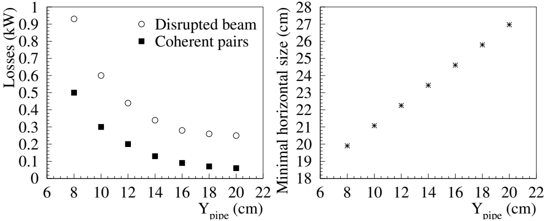

Estimation of the pipe and magnet dimensions (3)

If Y_{pipe} is the same in the three post-collision magnets, the losses are 6.1 kW and 35.6 kW in the 2nd and 3rd dipoles. To keep the losses below 1 kW per magnet, Y_{pipe} must be 37 cm and 68 cm in the 2nd and 3rd dipoles.

An alternative solution is to install collimators between two consecutive dipoles.

Element	X_{pipe} (in cm)	Y_{pipe} (in cm)	Losses in kW (disrupted beam)	Losses in kW (coherent pairs)	$2d + g$ (in cm)
Magnet 1	4.2	20.0	0.25	0.06	27.0
Collimator 1/2	4.6	10.0	0.62	0.47	-
Magnet 2	5.0	30.0	0.57	0.27	33.7
Collimator 2/3	5.4	20.0	3.98	2.19	-
Magnet 3	5.8	40.0	0.68	0.09	40.3

Beam profiles downstream the extraction magnets

Most of the particles that are found at the exit of the third post-collision magnet carry more than 10% of the nominal beam energy.

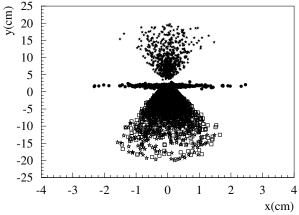

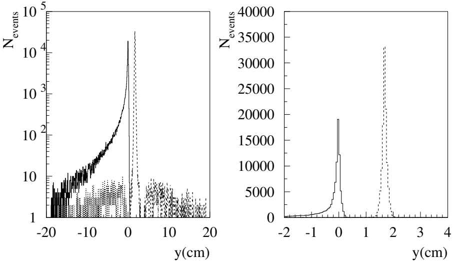

Future investigations

- The particles of the coherent pairs with the wrong-sign charge should be extracted and transported to a separate dump. This beam can be useful for diagnostics purposes.
- The beamstrahlung photons and the charged particles (disrupted beam + half of the coherent pairs) can be either transported and analysed separately, or brought together to a common dump (see next slides).
- Do we need soft focusing to reduce the vertical beam size without extra collimators?
- How do we measure the beam properties downstream the extraction magnets? Do we want a secondary focus point?

Contents

A post-collision chicane for CLIC

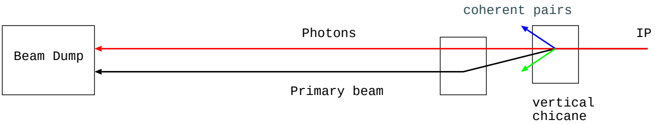

The vertical chicane consists of the 3 extraction magnets studied previously, followed by a bend in the opposite direction (also with 3 magnets). The dump is located about 100 m downstream of the chicane. No extra focusing is used.

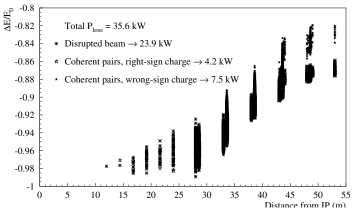

Stress at the dump window

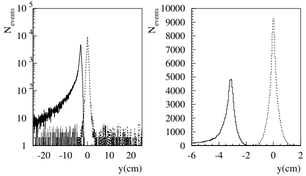

Beam profiles at the dump window

The stress on the window is:
$\sigma = 0.49 \Delta p R^2 / d^2$.

We use $\Delta p = 1$ bar, $R = 10$ cm and $d = 3$ mm $\rightarrow \sigma = 55$ MPa, well below the stress limit of 200 MPa for copper.

Only ionization losses will occur in the window, with a magnitude $(dE/dx)/\rho = 2.35$ MeV/cm^{2}g.

Instantaneous temperature rise at the dump window

The instantaneous temperature rise due to the impact of a train of (undisrupted) bunches with $N_{train} = 220 \times 2.56\,10^9$ particles generates a temperature rise $\hat{T}$:

$$\hat{T} = \frac{1}{\rho}\left(\frac{dE}{dx}\right)\frac{N_{train}e}{2\pi\sigma_x\sigma_y C_v} = 10.5\,\mathrm{K}$$

The cyclic stress due to the temperature increase is modest:

$$\sigma_c = \alpha E \hat{T}/2 = 9.5\,\mathrm{MPa}$$

$E = 110\,\mathrm{GPa}$ is Young's modulus and $\alpha = 16.5 \times 10^{-6}/\mathrm{K}$ is the thermal expansion coefficient.

Temperature evolution at the dump window

At a rate of 150 Hz, bunch trains heat the window at the center, from where the heat diffuses to the edge (fixed temperature of 37 C).

We solved the corresponding heat conduction equation with a periodic excitation:

$$\frac{\partial T}{\partial t} = \frac{D}{r}\frac{\partial}{\partial r} r \frac{\partial T}{\partial r} + \sum_n \hat{T}\delta(t - n\Delta t),$$

where the thermal diffusion constant is $D = 1.1\,\mathrm{cm}^2/\mathrm{s}$ for copper.

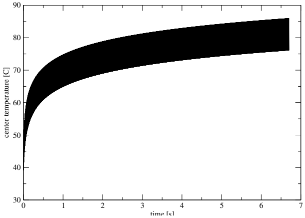

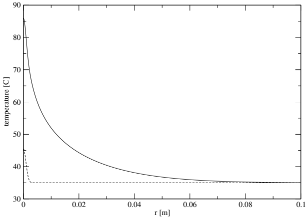

Interferometric thermometer at the dump

Use two windows spaced by 2 mm and fill the thin region between them with a laminar flowing sheet of water.

If the water flows horizontally, monitor its vertical temperature distribution, e.g. with an interferometric thermometer. This will provide a signal related to the vertical energy deposition and information on the angular divergence at the interaction point.

See V. Ziemann, *Ideas for an Interferometric Thermometer*, accepted for publication in Nucl. Inst. and Meth. A, 2006.

Conclusion and outlooks

- We presented a design of three extraction magnets to separate the various components of the outgoing CLIC beam. Collimators are used to limit the power losses in the magnet and thereby to allow a reasonable magnet size.
- As a possible extension, we presented a design of a vertical chicane and studied the stress and temperature rise at the dump window.
- More studies are planned: complete separation of e/γ, use of soft focusing to reduce the beam sizes, transport of the wrong-sign charged particles, etc.
- Study the impact of the beam losses on the magnet and collimator design, as well as the effect of back-scattered particles on the detector background.